SPATIAL VARIATIONS IN SEISMIC MOTIONS

G.P. NAIR and J.J. EMERY
Department of Civil Engineering and Engineering Mechanics,
McMaster University, Hamilton, Ontario, L8S 4L7

ABSTRACT

A method for evaluating the spatial variations in seismic motions for a linear, homogeneous and horizontally stratified soil layer system is presented. The procedure accounts for: the focal depth and the epicentral distance; the corresponding angle of incidence; and, the relative contributions of both shear and Rayleigh waves. The inclined propagation of shear waves is studied using the multiple reflection refraction theory. The range of possible values of Rayleigh wave phase velocity in the soil layer system is determined, and using an averaging procedure the Rayleigh wave amplification factors are computed. The influences of various factors on the spatial variations in seismic response are discussed. The method is general so that it can be used for various problems involving spatial motion computations. The application of the method in computing the responses of a soil-pile system is described and some typical results given.

INTRODUCTION

Records of ground motions during recent earthquakes have indicated that there are spatial variations in seismic motions. The earthquake motions in the soil at any depth for a particular location depend on the nature of incoming seismic waves in addition to certain other factors. These waves travel through a number of geologic formations and undergo multiple reflections, refractions and dispersions. The types of waves and their relative contributions to the ground motion are dependent on the epicentral distance and the focal depth (Dezfulian and Seed 1971; Tsai 1969; Yamahara 1970). At a site in the near-earthquake region, the motions will be comprised of several waves propagating at various velocities and spanning a wide range of frequencies (Trifunac and Brune 1970). In contrast, at a distant site the contributions to the motion by the various types of seismic waves will not overlap and it is not necessary to consider their combined effect.

The nature of seismic waves is usually not well defined, and both the geometric and elastic properties of the surface layers are often poorly delineated

(Dezfulian and Seed 1971). Therefore, it is necessary to commence this theoretical study with a relatively simple, idealized model consisting of linear, homogeneous and horizontally stratified soil layers. Then, the layer boundaries are planes extending to infinity in both horizontal directions. Although shear waves are the most important components, the analysis of several typical seismic records indicates that a significant portion of the earthquake ground motion consists of surface waves (Trifunac and Brune 1970). Fig. 1 gives an idealized system showing the relation between the focal depth of the source, the epicentral distance of the station and the wave paths. The arrival time for each type of wave and the corresponding contribution to the total ground motion are dependent on the focal depth, the epicentral distance and the effects of multiple reflections, refractions and dispersions along the various paths. For sites of moderate epicentral distance, the surface waves are usually masked by the shear waves and as a result, a small portion of the accelerations may be attributed to the surface waves. Rayleigh waves are the most significant among all surface waves (Richart et al 1970). Further, in the case of near sites, the direction of shear wave

propagation may be inclined. Thus, the usual assumption of energy transfer by means of vertically propagating shear waves is valid only for large epicentral distances.

A method for computing the three components of earthquake motion at a specified location is presented. The spatial variations in seismic motions are computed using wave propagation theory and assuming that the earthquake energy is transferred through the soil layers by both Rayleigh waves and inclined shear waves. Spatial variations in motion are compared for various epicentral distances and wave propagation assumptions. It is found that the surface waves (Rayleigh waves) make a significant contribution to the response at near sites, while the effect of inclining the shear wave is of secondary importance. The application of the method is described when examining the response of a typical soil-pile system.

RAYLEIGH WAVE PROPAGATION

Rayleigh waves may be caused by both types of body waves (dilatational and shear) and, unlike body waves, their velocity depends on the wave frequency and the

wave length in addition to the soil properties (Richart et al 1970). These waves propagate as plane waves and as a result, the displacements are independent of the transverse direction. The relationships for the velocities and stresses due to Rayleigh wave propagation in an elastic soil layer system may be established in terms of the phase velocity c and the wave number k_w of plane Rayleigh waves, using the methods developed by Thomson (1950) and Haskell (1953).

The body waves generated at the origin are complex in nature and these waves, after travelling through different soil layers, result in a series of Rayleigh waves with different wave numbers propagating at different velocities. Although there is no straightforward method of assigning a value for either the wave number or the phase velocity, it is possible to specify bounds for the Rayleigh wave propagational velocity in a layered soil strata. If β_L is the lowest shear wave velocity in the soil layers and β_R is the shear wave velocity in rock, then the possible range for c is given by:

[1] $$0.93\beta_L \leq c \leq \beta_R$$

In this range, the phase velocity of the plane Rayleigh wave may assume any value depending on the wave number.

For any value of c the evaluation of k_w may be accomplished by means of the trial and error procedure given in Appendix II.

The responses of the various soil layers due to Rayleigh wave propagation may be expressed in terms of the surface responses using transfer functions. In order to evaluate these transfer functions, an averaging procedure is adopted. The various values of c within its possible range were considered, and it was found that only values of c for c/β_1 less than β_n/β_1 gave consistent and meaningful results by exhibiting the required decay of motions with depth. β_1 and β_n are the shear wave velocities in the surface layer and the lowest soil layer, respectively. The method of computation is as follows:

1. Compute the possible range for the values of c. Take a set of c-values at regular intervals in this range.

2. For each c-value, determine the wave number using the trial and error procedure given in Appendix II. For these values of c and k_w, calculate the functions F_1 and F_2 which are defined in Appendix II, and then the surface velocities, which satisfy the following relationship:

[2] $$\dot{w}_o/c = -(F_2/F_1)\ \dot{u}_o/c$$

where $\dot{w}_o$ and $\dot{u}_o$ are the particle velocities at the surface in the vertical and horizontal directions, respectively.

3. The horizontal response of the m^{th} interface is expressed by:

[3] $$\dot{u}_m/c = [(A_m)_{11} - (F_2/F_1)\ (A_m)_{12}]\ \dot{u}_o/c$$

where $(A_m)_{ij}$ is an element of the matrix $[A_m]$ defined in Appendix II and $\dot{u}_m$ is the horizontal particle velocity in the m^{th} interface. Then, the transfer function T_m for the m^{th} interface response in the horizontal direction is given by:

[4] $$T_m = (A_m)_{11} - (F_2/F_1)\ (A_m)_{12}$$

Using Eq. 4, all transfer functions T_o, T_1, ... , T_n are computed where the subscript indicates the interface number.

4. Similarly, for each other value of c in its range, evaluate k_w and the transfer functions T_o, T_1, ... , T_n.

5. For any interface m, the transfer function T_m is taken as the average value for the various values of c in its possible range. Finally, the transfer functions T_o, T_1, ... , T_n for the horizontal components of

the seismic responses of interfaces due to the propagation of Rayleigh waves are evaluated.

6. The procedure for computing the vertical transfer functions T_{vo}, T_{v1}, ... , T_{vn} is the same as that for evaluating T_o, T_1, ... , T_n with the only difference that T_{vm} is expressed as:

[5] $$T_{vm} = (A_m)_{21} - (F_2/F_1)\ (A_m)_{22}$$

INCLINED SHEAR WAVES

Extensive research has been carried out to determine the angle of incidence of earthquake motions (Suzuki 1932; Chandra 1972; Randall 1971). After observing the angle of incidence for about fifty earthquake cases at Hongo Japan, Suzuki (1932) concluded that the mean angle of incidence for these earthquakes at Hongo was 4°, its fluctuation being small. Fig. 2 shows the relationship between the angle of incidence, the epicentral distance and the focal depth.

Seismologists have developed a method for determining the incident angle of shear waves (Chandra 1972; Randall 1971). This method is based on a theoretical model of the upper mantle and suits distant sites. According to their findings, the ratio of the sine of

the incident angle to the shear wave velocity in a layer is a constant for a site for specified values of focal depth and epicentral distance, with the epicentral distance being the more important factor. Qualitatively it may be stated that the angle of incidence is only significant for short distances.

In the absence of accurate data, it is required to make some assumption regarding the angle of incidence. By choosing the surface layer velocity as 11200 fps (3420 m/s) in the earth model, Chandra (1972) computed the angle of incidence at the surface as approximately 36° for large distances. Allowing for a model adjustment factor of 1.5, the angle of incidence may be assumed as 54° for short distances. This corresponds to an angle of incidence θ_1 at the surface:

[6] $$\theta_1 = \text{Sin}^{-1} (0.000072\beta_1)$$

where θ_1 is in degrees and β_1 is in fps. For small values of θ_1, Eq. 6 may be reduced to the form:

[7] $$\theta_1 = \frac{\beta_1}{240}$$

where θ_1 is in degrees and β_1 is in fps. The angle of incidence at the surface is given by Eq. 7 for short and moderate distances; and is zero for large distances.

When an inclined shear wave meets an interface,

there are four resultant waves, namely, the transmitted shear wave, the reflected shear wave, the transmitted P-wave (dilatational body wave) and the reflected P-wave. As the angle of inclination decreases, the amplitude of the emitted P-waves tends to become unimportant. Therefore, it is reasonable in such cases to assume that only shear waves are emitted at an interface due to an incident shear wave.

When shear waves travel in an inclined direction, there is not only a time lag in the vertical direction, but also one in the horizontal direction. Thus, two locations at the same level and horizontally separated do not have an identical motion at any time t. Therefore it is required to clearly define the locations at which responses are to be computed. In a case where only layer responses are considered, the locations are taken along a vertical line. Then the response of layer interface k refers to the response of the point of intersection of this vertical line with the interface k.

IDEALIZED PATH OF SHEAR WAVE PROPAGATION

The idealized three dimensional soil medium is shown in Fig. 3. It is assumed that the shear waves that cause motions on the x-z plane are plane waves and

that these motions are independent of waves on the y-z plane. An idealized path of the wave propagation on the x-z plane is given in Fig. 4-a. The wave path in the k^{th} layer makes an angle of inclination θ_k with the vertical, and as the wave transmits upward into the $k\text{-}1^{th}$ layer, there occurs a deviation in its path at the boundary and the angle of inclination alters to θ_{k-1} in the $k\text{-}1^{th}$ layer. The deviation satisfies the relationship:

[8] $$\beta_k/\beta_{k-1} = \text{Sin } \theta_k/\text{Sin } \theta_{k-1}$$

A wave signal that moves upward and reaches the location O_k at any time t continues on its path and reaches the location O' at time $t+\Delta t$, where Δt is the time lag between O_k and O'. The difference in arrival times of the same wave signal at any two locations is termed the time lag between them.

The particle motions due to shear waves are in a direction normal to that of the wave propagation. Then, two locations O_{k-1} and O' in Fig. 4-b get excited simultaneously by the same wave signal. In order to mark all locations which have no time lag with respect to O_{k-1}, the procedure involves projecting the line O_{k-1} - O' both ways such that the direction of this extended line is normal to the wave path in any layer. Fig. 4-a shows

the locus of all such points which have zero time lag with respect to one another and this may be termed an isolag. It is important to note that the amplitudes of motions at these points are not equal because they are at different elevations.

In general, for any two locations in the soil medium, there is a time lag between them and this may be decomposed into a vertical time lag component and a horizontal time lag component. For example, if t_ℓ is the time lag between O_n and O_s in Fig. 4-a, then

[9] $$t_\ell = t_{v\ell} + t_{h\ell}$$

where $t_{v\ell}$ is the vertical time lag between O_n and O_s and $t_{h\ell}$ is the horizontal time lag between them.

RESPONSES OF LAYERED SOIL SYSTEMS TO SHEAR WAVES

The theory of multiple reflections and refractions may be utilized to compute the seismic responses of the layered soil system shown in Fig. 4-a. A typical interface between the k^{th} and $k+1^{th}$ layers as shown in Fig. 5-b is considered. The impedance ratio μ_k between two adjacent layers is defined by:

[10] $$\mu_k = \frac{\rho_k \beta_k}{\rho_{k+1} \beta_{k+1}}$$

where ρ is the appropriate layer density. When an upward wave signal is incident on this interface there is an upward transmission into the k^{th} layer and a downward reflection back into the $k+1^{th}$ layer. In the same way there is a downward transmission and an upward reflection when the incident signal is downward. The coefficients of upward reflection, downward reflection, upward transmission and downward transmission at interface k are respectively (Kobayashi and Kagami 1972):

$$(R_u)_k = (\mu_k - 1)/(1+\mu_k)$$

$$(R_d)k = (1-\mu_k)/(1+\mu_k)$$

[11] $$(T_u)_k = 2/(1+\mu_k)$$

$$(T_d)_k = 2\mu_k/(1+\mu_k)$$

When a wave travels upward, it takes some time for the wave to travel from the bedrock level to the various soil interfaces. Between two adjacent interface points such as O_k and O_{k-1}, corresponding to the layer k in Fig. 4, the time lag is:

[12] $$t_\ell = h'_k/\beta_k$$

where h'_k is h_k Cos θ_k, h being the appropriate layer thickness. For the layered soil system in Fig. 5-a the pertinent equations are:

$$R_1(t) = F_1(t-h'_1/\beta_1)$$

$$F_1(t) = (T_u)_1\ F_2(t-h'_2/\beta_2) + (R_u)_1\ R_1(t-h'_1/\beta_1)$$

$$R_2(t) = (R_d)_1\ F_2(t-h'_2/\beta_2) + (T_d)_1\ R_1(t-h'_1/\beta_1)$$

$$F_2(t) = (T_u)_2\ F_3(t-h'_3/\beta_3) + (R_u)_2\ R_2(t-h'_2/\beta_2)$$

...

$$R_k(t) = (R_d)_{k-1}\ F_k(t-h'_k/\beta_k) + (T_d)_{k-1}\ R_{k-1}(t-h'_{k-1}/\beta_{k-1})$$

[13] $$F_k(t) = (T_u)_k\ F_{k+1}(t-h'_{k+1}/\beta_{k+1}) + (R_u)_k\ R_k(t-h'_k/\beta_k)$$

...

$$R_n(t) = (R_d)_{n-1}\ F_n(t-h'_n/\beta_n) + (T_d)_{n-1}\ R_{n-1}(t-h'_{n-1}/\beta_{n-1})$$

$$F_n(t) = (T_u)_n\ F_{n+1}(t)$$

$$F_{n+1}(t) = \text{Base rock response}$$

where F_k and R_k are the transmitted and reflected components of the k^{th} interface response, respectively.

The values of response components F_k and R_k for the various layer interfaces at any time t are evaluated with the aid of their previous values which are known. Thus, the method is a step-by-step procedure and the components F_k and R_k may refer to displacements, veloc-

ities or accelerations. When the responses considered are the accelerations, the required equation is:

$$[14] \qquad \ddot{u}_k(t) = F_k(t-h'_k/\beta_k) + R_k(t)$$

where $\ddot{u}_k(t)$ is the acceleration at time t in the x direction.

If observed earthquake motions at the bed rock level are available, Eq. 13 may be used repeatedly to compute the earthquake motions at various interface points proceeding from bottom to top. However, there are only a few earthquake records available for the bed rock level while most others are records of motion at the surface. The method needs modification to simplfy the layer response computation based on the known surface response. Referring to the soil layer system shown in Fig. 6 the relevant equations are:

$$F_1(t) = R_1(t) = \text{half the surface response at time t}$$

$$F_2(t) = [(T_u)_1]^{-1} [F_1(t+h'_1/\beta_1) - (R_u)_1 R_1(t-h'_1/\beta_1)] \qquad [15]$$

$$R_2(t) = (R_d)_1 F_2(t) + (T_d)_1 R_1(t-h'_1/\beta_1)$$

...

$$F_k(t) = [(T_u)_{k-1}]^{-1} [F_{k-1}(t+h'_{k-1}/\beta_{k-1}) -$$

$$(R_u)_{k-1}\ R_{k-1}(t-h'_{k-1}/\beta_{k-1})]$$

$$R_k(t) = (R_d)_{k-1}\ F_k(t) + (T_d)_{k-1}$$

$$R_{k-1}(t-h'_{k-1}/\beta_{k-1})$$

$$F_n(t) = [(T_u)_{n-1}]^{-1}\ [F_{n-1}(t+h'_{n-1}/\beta_{n-1}) -$$

$$(R_u)_{n-1}\ R_{n-1}(t-h'_{n-1}/\beta_{n-1})]$$

$$R_n(t) = (R_d)_{n-1}\ F_n(t) + (T_d)_{n-1}$$

$$R_{n-1}(t-h'_{n-1}/\beta_{n-1})$$

$$F_{n+1}(t) = [(T_u)_n]^{-1}\ [F_n(t+h'_n/\beta_n)]$$

The acceleration at the top of the k^{th} layer is:

[16] $$\ddot{u}_k(t) = F_k(t) + R_k(t)$$

The response of the soil layers may be determined using Eq. 15 if the surface motions during an earthquake are known.

METHOD FOR SPATIAL MOTIONS

The computation of the three components of earthquake motions at certain specified locations may be accomplished by means of a three dimensional analysis. However, such a procedure is complicated and therefore a simpler method involving plane wave motions is

utilized. Certain broad assumptions are made in order to facilitate these computations:

1. The motions on the x-z plane are independent of the y direction, and similarly, the motions on the y-z plane are independent of x.

2. For distant sites, the vertical shear wave propagation assumption is valid. For near sites, the combined effect of Rayleigh waves and inclined shear waves is accounted for.

3. The propagation of shear waves and Rayleigh waves are independent of each other.

4. The angle of incidence in degrees for near sites is $\beta_1/240$ where β_1 is in fps.

5. Only shear waves are emitted at an interface due to an incident shear wave.

Computational Procedure

The computational procedure requires a clear identification of the various response locations. For this purpose a vertical line is taken as the reference as indicated in Fig. 3, and the horizontal distances (x and y coordinates) are measured from this line. Any point in space is then defined

by its x and y coordinates and the interface on which it lies. The following procedure for computing spatial motions is followed systematically:

1. For each point in the required set where motions are to be computed, list the x and y coordinates and the interface number corresponding to the point's location.
2. Determine the angle of incidence in degrees of the shear wave at the surface which is $\beta_1/240$ where β_1 is in fps when the site is near, and zero for a far site. Find the angles of inclination of the shear wave in the various layers using Eq. 8.
3. Compute the x directional time lag for each point with respect to the reference line O_n-O. Referring to Fig. 3, the time lag of P_k is measured with relation to O_k while that of P_{k-1} is ascertained with reference to O_{k-1}. As both P_k and P_{k-1} have the same x coordinate, the x directional time lags for both P_k and P_{k-1} are equal. In a similar way, the y directional time lags for the various points are determined.
4. For short epicentral distances, it may be assumed that the relative contribution of shear waves is 75%. When the ratio of the epicentral distance to

the focal depth reaches 5, only shear waves need be considered. For distances in between these limits, interpolation is required. Let the contribution of shear waves be denoted by ξ.

5. If there is any contribution due to Rayleigh waves ($\xi \neq 1$), then evaluate the transfer functions for interface responses due to Rayleigh wave propagation using the procedure given earlier. For the k^{th} layer, these transfer functions are T_k and T_{vk} for the horizontal and vertical motions. The response of the k^{th} layer as a result of Rayleigh wave motions at any time t may be computed as the product of $(1-\xi)$, its transfer function and the surface response at time t.

6. If the surface responses are available as data, then these motions are valid for the point O on the reference line (Fig. 4-a). Let S(t) be the excitation due to incident waves arriving at O at any time t. This excitation may be resolved into two portions, one due to shear wave propagation and the other due to Rayleigh waves. The portion of the excitation carried by shear waves is $\xi S(t)$ and the remaining portion $(1-\xi)S(t)$ is taken by Rayleigh waves. If instead of the surface response the base

motions are available, then they refer to the point O_n.

7. From the data for O_n or O, proceed and complete the response calculations for points such as O_k and O_{k-1} using shear wave propagation theory. The vertical time lag between the two adjacent interface points O_{k-1} and O_k is given by h'_k/β_k. If motions at O_n are available, then Eqs. 13 and 14 are applicable, while Eqs. 15 and 16 are to be used for the case of motions given at O. First the x direction motions (E-W direction) are computed for the entire period of the record. Let $\ddot{u}'_0(t)$, $\ddot{u}'_1(t)$, ... , $\ddot{u}'_n(t)$ be the computed x direction motions of interface points O, O_1, ... , O_n at time t. As Rayleigh waves were not yet accounted for, a correction is required in the values. Let $\ddot{u}_0(t)$, $\ddot{u}_1(t)$, ... , $\ddot{u}_n(t)$ be the corrected x direction motions at the interface points. Then the following relationships hold:

$$\ddot{u}_0(t) = \ddot{u}'_0(t)$$

$$\ddot{u}_1(t) = \xi\, \ddot{u}'_1(t) + (1-\xi)\, T_1\, \ddot{u}'_0(t)$$

$$[17] \quad \ddot{u}_k(t) = \xi\, \ddot{u}'_k(t) + (1-\xi)\, T_k\, \ddot{u}'_0(t)$$

$$\ddot{u}_n(t) = \xi\, \ddot{u}'_n(t) + (1-\xi)\, T_n\, \ddot{u}'_o(t)$$

There is a computational advantage in storing the pre-correction values of the x direction motions, namely, $\ddot{u}'_o(t)$, $\ddot{u}'_1(t)$, ... , $\ddot{u}'_n(t)$. In a similar way the y direction (N-S direction) motions $\ddot{v}'_o(t)$, $\ddot{v}'_1(t)$, ... , $\ddot{v}'_n(t)$ are computed and stored. The relationships in Eq. 17 hold for y direction motions if u is replaced by v in all expressions.

8. The spatial motions at the various required locations are computed one by one. For example, if the responses at O_k and P_k in Fig. 3 are required, then they may be computed using the following relationships:

$$\ddot{u}_{ok}(t) = \xi\, \ddot{u}'_k(t) + (1-\xi)\, T_k\, \ddot{u}'_o(t)$$

$$\ddot{v}_{ok}(t) = \xi\, \ddot{v}'_k(t) + (1-\xi)\, T_k\, \ddot{v}'_o(t)$$

$$\ddot{w}_{ok}(t) = \xi \tan\theta_k\, [\ddot{u}'_k(t) + \ddot{v}'_k(t)] + (1-\xi)$$

$$T_{vk}[\ddot{u}'_o(t) + \ddot{v}'_o(t)] \qquad [18]$$

$$\ddot{u}_{pk}(t) = \xi\, \ddot{u}'_k(t-t_{hp}) + (1-\xi)\, T_k\, \ddot{u}'_o(t-t_{hp})$$

$$\ddot{v}_{pk}(t) = \xi\, \ddot{v}'_k(t-t_{hp}) + (1-\xi)\, T_k\, \ddot{v}'_o(t-t_{hp})$$

$$\ddot{w}_{pk}(t) = \xi \tan \theta_k [\ddot{u}_k(t-t_{hp}) + \ddot{v}'_k(t-t_{hp})]$$

$$+ (1-\xi)\, T_{vk}\, [\ddot{u}'_o(t-t_{hp}) + \ddot{v}'_o(t-t_{hp})]$$

ILLUSTRATIVE EXAMPLES

The influence of the epicentral distance and the focal depth on soil layer amplification is indicated by considering the four layer system (System 2) described in Table 1. When the ratio of the epicentral distance to the focal depth exceeds 5, the site is considered as distant. A computer program has been developed to facilitate the computation of the responses of the soil interface reference points such as 0, 0_1, ... , 0_n in Fig. 4-a due to the propagation of Rayleigh waves and inclined shear waves. The E-W component of the motion for the first twelve seconds during the Olympia Earthquake, 1949 was fed in as input at the base rock level and the motions at interface points have been computed using this program. Fig. 7 shows the surface responses of this system for three specific cases:

1. Nearby location; contribution of Rayleigh waves considered as 25% with the remaining contribution from the inclined propagation of shear waves.

2. Nearby location; inclined propagation of shear waves.
3. Distant location; vertical propagation of shear waves.

These results show that the response amplification due to soil layering is greater in magnitude when the contribution of Rayleigh waves is accounted for. The difference in the response curves for the near and distant sites is small when only the shear waves are considered in the computation.

The importance of spatial seismic motions is illustrated by studying the responses at different locations of the three layer system (System 1) described in Table 1. In order to accomplish this a computer program has been developed which can account for the inclined propagation of shear waves and the Rayleigh wave propagation. The variations in spatial motions are demonstrated by considering four locations on the x-z plane; locations 1 and 2 are at the bed rock level and at a distance of 50 ft (15.24 m) apart, while locations 3 and 4 are at the surface and directly above 1 and 2 respectively. Fig. 8 shows the responses at these locations due to the E-W component of accelerations for the first 0.5 second during the El Centro

Earthquake 1940, which was fed in at the bed rock level. It is obvious from this example that motions at the same levels are practically identical, except for a time lag between these motions.

RESPONSES OF A SOIL-PILE SYSTEM

The method for spatial motion computations is general so that it can be used for a variety of problems. Its application in studying the response of a soil-pile system with the finite element method illustrates a major class of problems that can be considered. Using the theory of spatial variations in seismic motions, the absolute boundary accelerations of the system are computed first. What remains to be considered is a computational procedure for evaluating the unknown responses at interior locations including the pile cap, which will satisfy boundary compatibility and equilibrium of the system. The dimensions of the soil-pile system are chosen so that free field conditions can be assumed at the boundary. The length of the pile, the total depth of soil layers and the shear wave velocities as well as the predominant period of ground motions are important factors in defining these dimensions of the system.

The soil-pile system is an axisymmetric structure and the nonsymmetric excitation of the system can be separated into a series of analyses in different harmonics. Thus, the required data for the final dynamic analysis are the radial, circumferential and axial components of the absolute boundary accelerations in each significant harmonic. Fig. 9-a shows the discretized structure and the boundary nodes at which these coefficients are specified. Of these nodes, 1 to 5, 15, 24, 29 and 59 lie on interfaces between different soil layers. The remaining nodes, namely, 6, 33 and 39 are between interfaces. The acceleration coefficients at node 15 in the various harmonics for any time t are described as an example. In order to accomplish this, it is necessary to consider the boundary accelerations at all points along the nodal ring 15 as shown in Fig. 9-b. Once the cylindrical components of accelerations at any time t at all points along the nodal ring 15 are known, then it is possible to find the acceleration coefficients in each significant harmonic at that time. However, it is not possible to use a general expression for accelerations along a nodal ring and then find the required acceleration coefficients at the node in the various harmonics. There-

fore, the accelerations at a few selected points are first determined. It is more convenient to have 12, 16 or 8 points so that the averaging is adequate. The radial, circumferential and axial components of accelerations at time t for the 12 selected points (spaced at regular angular distances of 30° as shown in Fig. 9-c) along the nodal ring are computed. Then the coefficients of acceleration in the different harmonics at node 15 are computed by means of an averaging procedure.

The boundary acceleration coefficients in the various harmonics are used as input for the final dynamic analysis which utilizes the finite element method. The dynamic analysis is carried out using a step-by-step procedure incorporating the linear acceleration method (Wilson and Clough 1962). The response of a 60 ft (18.29 m) long pile, 1.25 ft (0.38 m) in diameter, founded in 140 ft (42.67 m) of sand overlying bed rock was considered. This response was computed for different earthquakes and for different wave propagation assumptions. For comparison purposes, the pile in dry sand was considered for four specific cases:

1. Pile at a location near the source - travelling wave solution; contribution of Rayleigh

waves considered as 25% with the remaining contribution from the inclined propagation of shear waves.

2. Pile at a location near the source - travelling wave solution; inclined propagation of shear waves.
3. Pile at distant location - travelling wave solution; vertical propagation of shear waves.
4. Pile at distant location - rigid base solution; assumption that all points on the boundary of the soil-pile system move simultaneously.

Three different earthquakes were used in this study: Olympia Earthquake, 1949; El Centro Earthquake, 1940; and, accelerograms from the Pacoima dam site recorded during the San Fernando Earthquake, 1971.

Fig. 10 gives a comparison of the responses of the pile cap for the different assumptions during the San Fernando Earthquake. It can be seen that the rigid base solution under estimates the motions. The maximum acceleration using the rigid base solution is 14.22 ft/sec^2 (4.33 m/sec^2) while its values are 22.12, 20.65 and 18.30 ft/sec^2 (6.74, 6.29 and 5.58 m/sec^2) respectively

for cases 1, 2 and 3. The results are similar for the other two earthquakes and Table 2 gives the absolute maximum accelerations of the pile cap for the four cases during these earthquakes. The presence of the pile is beneficial as anticipated. When the epicentral distance decreased, the response of the soil-pile system increased. The data clearly indicate that a travelling wave solution is required to estimate the responses of the system, as otherwise the response is under estimated.

SUMMARY AND CONCLUSIONS

In the computation of the seismic response of structures, the effects of travelling seismic waves are usually accounted for by assuming that the earthquake energy is only carried by vertically propagating shear waves, or that the structure rests on a rigid, uniform base. A survey of field observations and computations by geophysicists show that the direction of wave propagation is inclined for most sites where seismic effects are significant. Many strong motion records for near sites reveal that a part of these motions are associated with surface waves. For this reason, the spatial

variations in seismic motions were studied taking into account the inclined propagation of shear waves and the presence of Rayleigh waves which are the most important of the surface waves. Certain broad assumptions were made with regard to the relative contributions of these waves, the angle of incidence, the decomposition of waves at soil interfaces and the time lags in motions for various site distances. The inclined shear wave propagation was accounted for by extending the method of multiple reflections and refractions. The Rayleigh wave amplification was considered in the frequency domain by assuming that these waves are uniformly spread in the anticipated range of phase velocities. Using these methods, it was possible to compute the seismic motion record in the three directions at any points. These seismic motion records can then be used as the boundary conditions for the solution of relatively complex soil-structure interaction problems.

ACKNOWLEDGMENTS

The research reported is part of a study supported by the Commonwealth Scholarship and Fellowship Plan (Association of Universities and Colleges of Canada).

Computer time provided by the McMaster University Science and Engineering Research Board is also gratefully acknowledged.

Chandra, U. 1972. Angles of incidence of S waves. Bull. Seismol. Soc. Am., 62(4), pp. 903-915.

Dezfulian, H., and Seed, H.B. 1971. Response of non-uniform soil deposits to travelling seismic waves. J. Soil Mech. Found. Div., A.S.C.E., 97(SM1), pp. 27-46.

Haskell, N.A. 1953. The dispersion of surface waves on multilayered media. Bull. Seismol. Soc. Am., 43 (1), pp. 17-34.

Kobayashi, H., and Kagami, H. 1972. A method for local seismic intensity zoning maps. Proc. Int. Conf. Microzonation for Safer Constr. Res. Applic., 2, Seattle, Wash., pp. 513-528.

Oliver, J., and Ewing, M. 1957. Higher modes of continental Rayleigh waves. Bull. Seismol. Soc. Am., 47(3), pp. 187-203.

Randall, M.J. 1971. Revised travel time table for S. Geophys. J. 22, pp. 229-234.

Richart, F.E., Woods, R.D., and Hall, J.R. 1970. Vibrations of Soils and Foundations. Prentice-Hall, Inc., Englewood Cliffs, N.J.

Sezawa, K. 1927. Dispersion of elastic waves propagated on the surface of stratified bodies and on

curved surfaces. Bull. Earthq. Res. Inst., 3, pp. 1-18.

Suzuki, T. 1932. On the angle of incidence of the initial motion observed at Hongo and Mitaka. Bull. Earthq. Res. Inst., 10, pp. 517-535.

Thomson, W.T. 1950. Transmission of elastic waves through a stratified solid medium. J. Appl. Phys., 21, pp. 89-93.

Trifunac, M.D., and Brune, J.N. 1970. Complexity of energy release during the Imperial Valley, California Earthquake of 1940. Bull. Seismol. Soc. Am., 60(1), pp. 137-160.

Tsai, N.C. 1969. Influence of local geology on earthquake ground motion. Ph.D. thesis, Calif. Inst. Tech., Pasadena, Calif.

Wilson, E.L., and Clough, R.W. 1962. Dynamic response by step-by-step analysis. Proc., Symp. Use of Computers in Civ. Eng., Lisbon, Portugal, No. 45, pp. 45.1-45.14.

Yamahara, H. 1970. Ground motions during earthquakes and the input loss of earthquake power to an excitation of buildings. Soils and Found., 10(2), pp. 145-161.

Appendix I - Notation

The following symbols are used in this paper:

$[A]$ = matrix relating n^{th} interface response due to Rayleigh wave propagation

A_{ij} = elements of $[A]$

$[A_n]$ = same as $[A]$

$[A_m]$ = matrix relating interface responses due to Rayleigh wave propagation defined by Eq. 19

$(A_m)_{ij}$ = elements of $[A_m]$

$[a_m]$ = matrix relating interface responses due to Rayleigh wave propagation defined by Eq. 20

$(a_m)_{ij}$ = elements of $[a_m]$

c = Rayleigh wave propagational velocity

$F_k(t)$ = transmitted component of k^{th} interface response at time t

F_1, F_2, F_3, F_4 = functions used in Rayleigh wave propagation defined by Eq. 21

h_k = thickness of layer k

h'_k = $h_k \text{ Cos } \theta_k$

k_w = wave number

L = wave length

P_m = function used in Rayleigh wave propagation defined by Eq. 18-d

Q_m = function used in Rayleigh wave propagation defined by Eq. 18-d

R_d = downward reflection coefficient

$R_k(t)$ = reflected component of k^{th} interface response at time t

R_u = upward reflection coefficient

r_{am} = function used in Rayleigh wave propagation defined by Eq. 18-a

r_{bm} = function used in Rayleigh wave propagation defined by Eq. 18-b

r_m = function used in Rayleigh wave propagation defined by Eq. 18-c

$S(t)$ = excitation due to incident wave at time t

T_d = downward transmission coefficient

T_m = transfer function for horizontal response of the m^{th} interface due to Rayleigh wave propagation

T_u = upward transmission coefficient

T_{vm} = transfer function for vertical response of the m^{th} interface due to Rayleigh wave propagation

t = time

$t_{h\ell}$ = horizontal time lag

t_ℓ = time lag

$t_{v\ell}$ = vertical time lag

$\ddot{u}_o$ = particle velocity at the surface in x direction

$\dot{u}_m$ = particle velocity at the m^{th} interface in x direction

$\ddot{u}_k(t)$ = acceleration in x direction due to the propagation of Rayleigh waves and inclined shear waves

$\ddot{u}'_k(t)$ = acceleration in x direction due to the propagation of shear waves alone

v = particle displacement in the circumferential or y direction

$\ddot{v}_k(t)$ = acceleration in y direction due to the propagation of Rayleigh waves and inclined shear waves

$\ddot{v}'_k(t)$ = acceleration in y direction due to the propagation of shear waves alone

$\dot{w}_o$ = particle velocity at the surface in z direction

α = P-wave velocity

β = shear wave velocity

β_L = lowest shear wave velocity in the

soil layers

β_R = shear wave velocity in rock

θ_k = angle of inclination of shear wave in the k^{th} layer

μ = impedance ratio

ξ = contribution of shear waves in the response

ρ = mass density

ω = frequency in radians/second

Superscripts

. = first derivative with respect to time

.. = second derivative with respect to time

Subscripts

h = horizontal direction

k = layer or interface k

ℓ = lag

m	=	layer or interface m
n	=	layer n, lowest soil layer or interface n
v	=	vertical direction

Appendix II - Layer Matrices and Determination of Rayleigh Wave Number

This appendix gives the functions and matrices used for studying the Rayleigh wave propagation through soil layers, and describes a computational procedure for determining the wave number k_w for a specified phase velocity c.

1. Functions and Matrices

The various layers and interfaces are shown in Fig. 11.

The details of the m^{th} layer are:

ρ_m = density

h_m = thickness

β_m = shear wave velocity

α_m = dilatational wave velocity

$k_w = \omega/c = 2\pi/L$ = wave number

L = wave length

[18-a]
$$r_{am} = \begin{cases} +[(c/\alpha_m)^2 - 1]^{1/2} & \text{if } c>\alpha_m \\ -i[1 - (c/\alpha_m)^2]^{1/2} & c<\alpha_m \end{cases}$$

$$r_{bm} = \begin{cases} +[(c/\beta_m)^2 - 1]^{1/2} & \text{if } c > \beta_m \\ -1[1 - (c/\beta_m)^2]^{1/2} & c < \beta_m \end{cases}$$

[18-c] $$r_m = 2(\beta_m/c)^2$$

[18-d] $$\begin{cases} P_m = k r_{am} h_m \\ Q_m = k r_{am} h_m \end{cases}$$

The matrix $[A_m]$ is defined by:

[19] $$[A_m] = [a_m]\,[a_{m-1}] \ldots\ldots [a_1]$$

where the elements of the matrix $[a_m]$ are:

[20]
$$(a_m)_{11} = r_m \cos P_m - (r_{m-1}) \cos Q_m$$

$$(a_m)_{12} = i[(r_{m-1}) r_{am}^{-1} \sin P_m + r_m r_{\beta m} \sin Q_m]$$

$$(a_m)_{13} = -(\rho_m c^2)^{-1} (\cos P_m - \cos Q_m)$$

$$(a_m)_{14} = i\,(\rho_m c^2)^{-1} (r_{am}^{-1} \sin P_m + r_{\beta m} \sin Q_m)$$

$$(a_m)_{21} = -\,i[r_m r_{am} \sin P_m + (r_{m-1})\, r_{\beta m}^{-1} \sin Q_m]$$

$$(a_m)_{22} = -(r_{m-1}) \cos P_m + r_m \cos Q_m$$

$$(a_m)_{23} = i\,(\rho_m c^2)^{-1} (r_{am} \sin P_m + r_{\beta m}^{-1} \sin Q_m)$$

$$(a_m)_{24} = (a_m)_{13}$$

$$(a_m)_{31} = \rho_m c^2\, r_m\, (r_{m-1})(\cos P_m - \cos Q_m)$$

$$(a_m)_{32} = i\ \rho_m c^2[(r_{m-1})^2\ r_{am}^{-1} \sin P_m + r_m^2\ r_{\beta m} \sin Q_m]$$

$$(a_m)_{33} = (a_m)_{22}$$

$$(a_m)_{34} = (a_m)_{12}$$

$$(a_m)_{41} = i\ \rho_m c^2\ [r_m^2\ r_{am} \sin P_m + (r_{m-1})^2\ r_{\beta m}^{-1} \sin Q_m]$$

$$(a_m)_{42} = (a_m)_{31}$$

$$(a_m)_{43} = (a_m)_{21}$$

$$(a_m)_{44} = (a_m)_{11}$$

By letting $[A] = [A_n] = [a_n] \ldots [a_2]\ [a_1]$, the functions F_1, F_2, F_3 and F_4 may be written as:

$$F_1 = r_n\ r_{an}\ A_{12} + (r_{n-1})\ A_{22} - r_{an}\ A_{32}/\rho_n c^2 + A_{42}/\rho_n c^2$$

$$F_2 = r_n\ r_{an}\ A_{11} + (r_{n-1})\ A_{21} - r_{an}\ A_{31}/\rho_n c^2 + A_{41}/\rho_n c^2$$

[21]

$$F_3 = -(r_{n-1})\ A_{12} + r_n\ r_{bn}\ A_{22} + A_{32}/\rho_n c^2 + r_{bn}\ A_{42}/\rho_n c^2$$

$$F_4 = -(r_{n-1})\ A_{11} + r_n\ r_{bn}\ A_{21} + A_{31}/\rho_n c^2 + r_{bn}\ A_{41}/\rho_n c^2$$

2. Computational Procedure for the Wave Number

The numerical computation of the wave number k_w corresponding to the phase velocity c of Rayleigh waves is carried out by a trial and error procedure. The steps involved in the procedure are followed systematically.

1. From the available data, tabulate quantities such as Poisson's ratio, mass density, layer thickness and wave velocity for each layer.

2. It is usually convenient to take the thickness h_1 of the first layer as the unit of length, ρ_1 as the unit of density and β_1 as the unit of velocity. The properties of the other layers may then be expressed in dimensionless form. The computations then give a relationship between dimensionless quantities kh_1 and c/β_1.

3. For any phase velocity c, compute the quantities r_m, r_{am} and r_{bm}, P_m, Q_m, etc. for each layer.

4. It is possible to make a preliminary estimate of the value of k_w for the chosen value of c such that this value may be within an order of magnitude of the correct value. For this purpose, Sezawa's curves (1927) for the two-layer case or curves provided by

Oliver and Ewing (1957) may be used. If the computation is carried out on a computer, k_w may be given the value of unity to start with.

5. With the chosen value of c and the assumed value of k_w, compute the functions F_1, F_2, F_3 and F_4 in Eq. 21, and the ratios F_1/F_2 and F_3/F_4.

6. If $(F_1/F_2 - F_3/F_4)$ is very small in magnitude compared to F_1/F_2 or F_3/F_4, then the assumed value for k_w is acceptable.

7. If the difference is significant, select another value of k_w and repeat the procedure until the appropriate k_w for the chosen c is established.

TABLE 1. DATA FOR LAYERED SOIL SYSTEMS

SYSTEM	LAYER NUMBER	LAYER THICKNESS ft (m)	DENSITY lb/ft^3 (kg/m^3)	SHEAR WAVE VELOCITY fps (m/s)
1	1	150	110	900
		(45.7)	(1760)	(274)
	2	150	120	2000
		(45.7)	(1920)	(610)
	3	175	140	4000
		(53.3)	(2240)	(1220)
	Bed Rock		145	7500
			(2320)	(2286)
2	1	150	110	900
		(45.7)	(1760)	(274)
	2	75	120	2000
		(22.8)	(1920)	(610)
	3	100	130	3000
		(30.5)	(2080)	(915)
	4	150	140	4000
		(45.7)	(2240)	(1220)
	Bed Rock		145	7500
			(2320)	(2286)

TABLE 2. ABSOLUTE MAXIMUM ACCELERATIONS OF THE PILE CAP, FT/SEC^2 (M/SEC^2)

Earthquake	Case 1	Case 2	Case 3	Case 4	Base Rock	Surface at distant location (input)
Olympia, 1949	2.81	2.50	2.35	1.82	1.53	4.94
	(0.85)	(0.76)	(0.72)	(0.55)	(0.47)	(1.51)
El Centro, 1940	5.53	5.09	4.47	3.42	3.11	10.17
	(1.69)	(1.55)	(1.36)	(1.04)	(0.95)	(3.10)
San Fernando, 1971. (Pacoima Dam)	22.12	20.65	18.30	14.22	12.35	40.30
	(6.74)	(6.29)	(5.58)	(4.33)	(3.76)	(12.28)

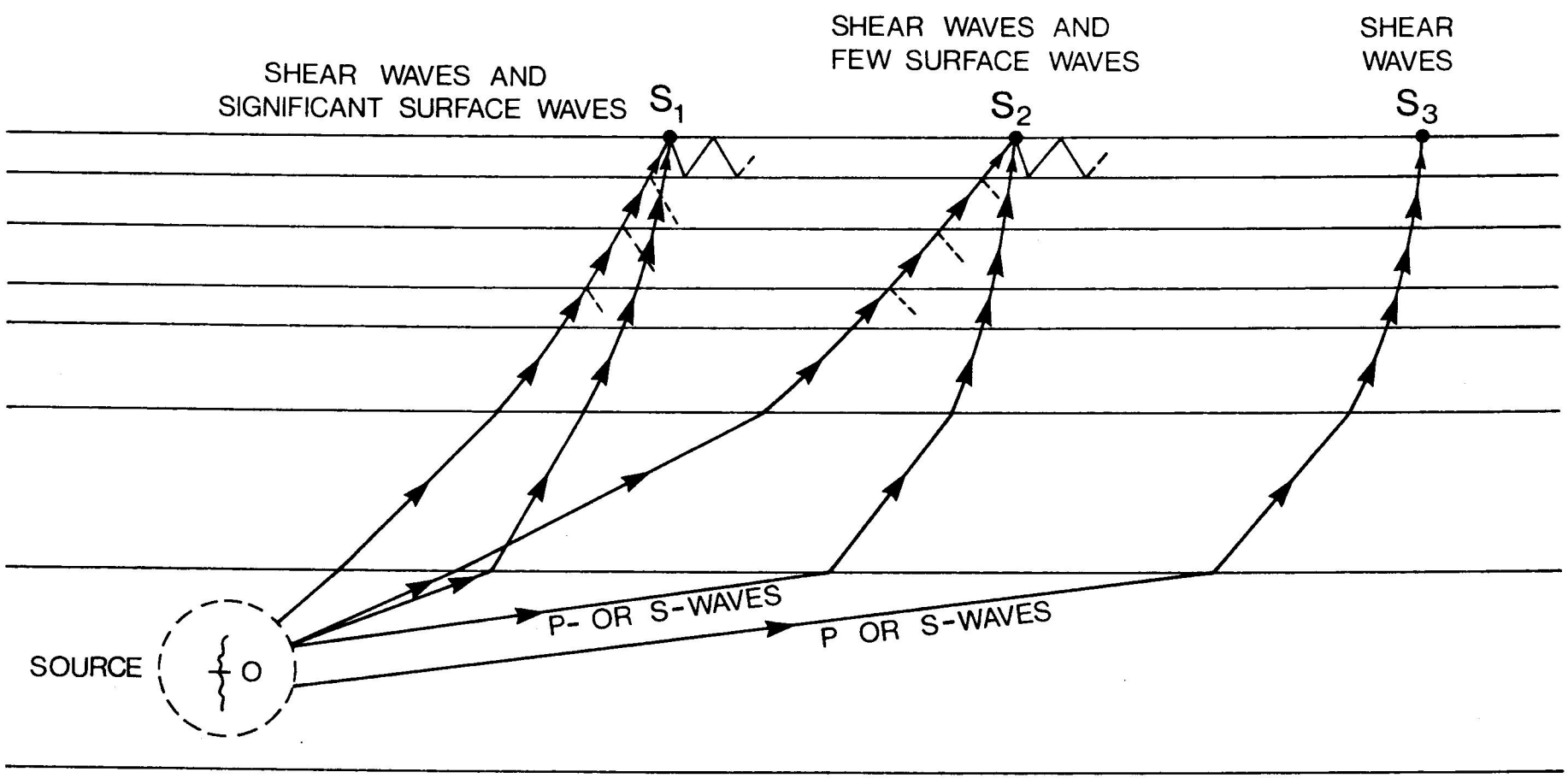

FIG. 1 IDEALIZED SYSTEM SHOWING FOCAL DEPTH, EPICENTRAL DISTANCE AND WAVE PATHS (TSAI 1969)

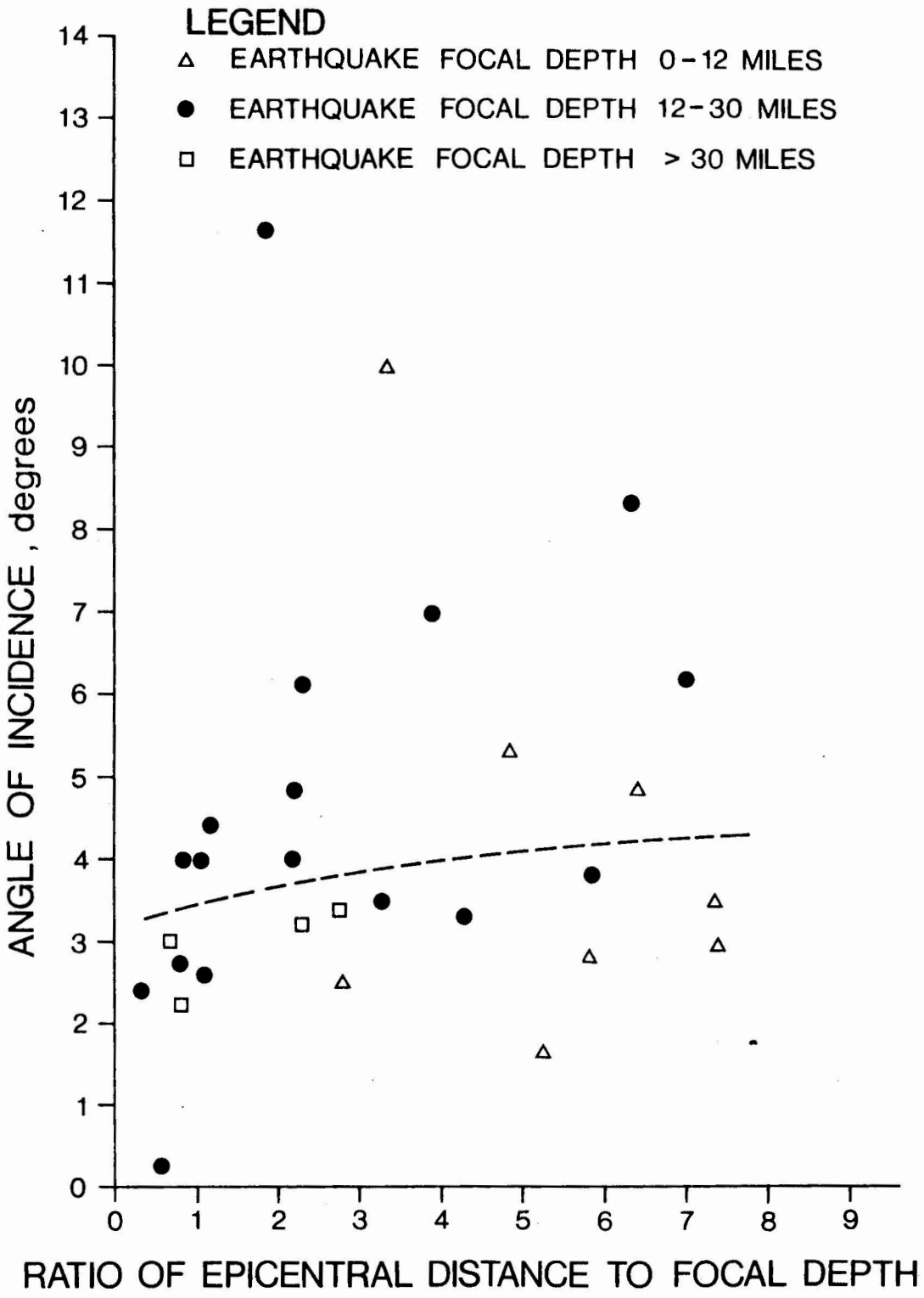

FIG. 2 RELATION BETWEEN ANGLE OF INCIDENCE, EPICENTRAL DISTANCE AND FOCAL DEPTH (SUZUKI 1932)

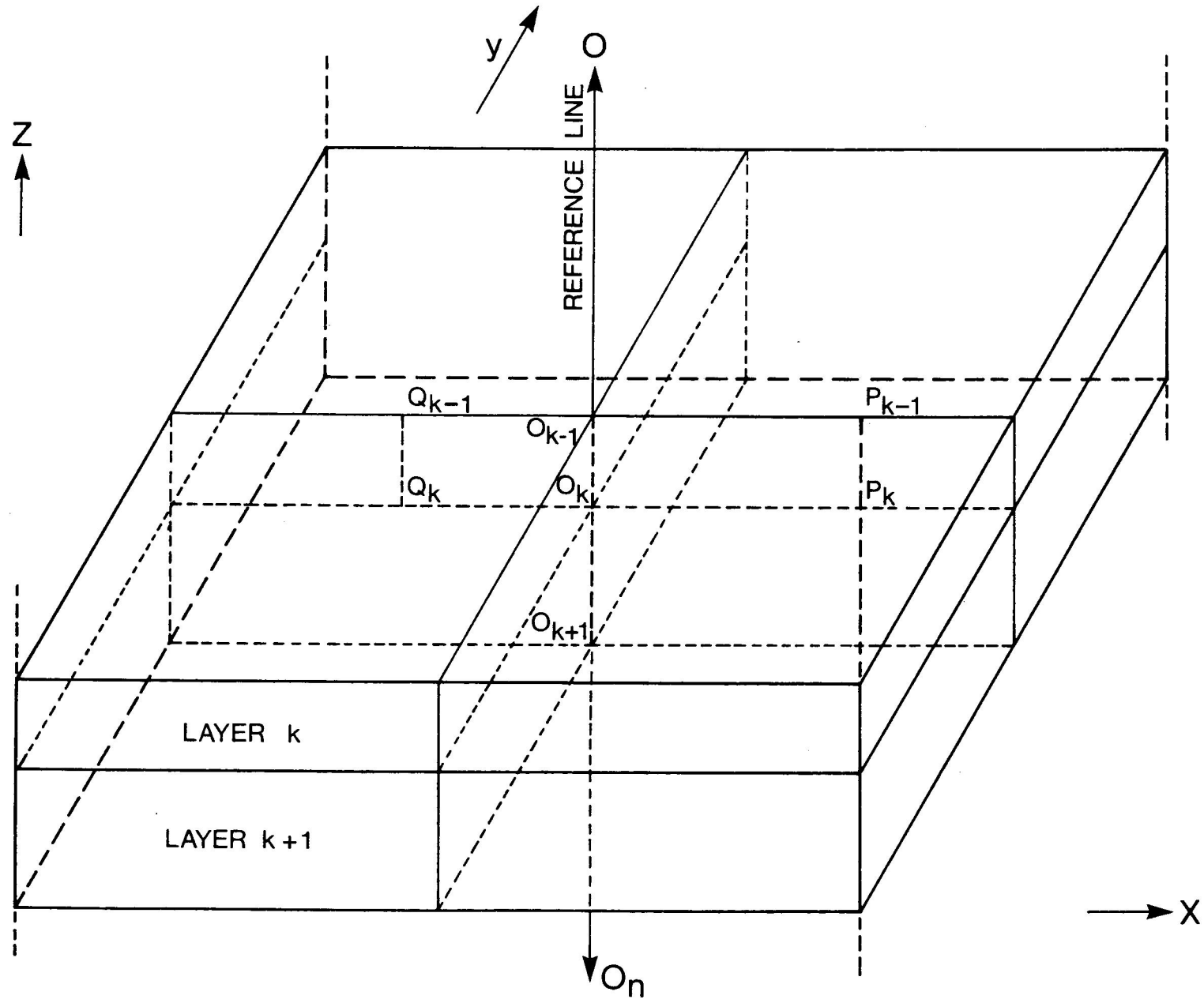

FIG. 3 IDEALIZED THREE DIMENSIONAL SOIL MEDIUM

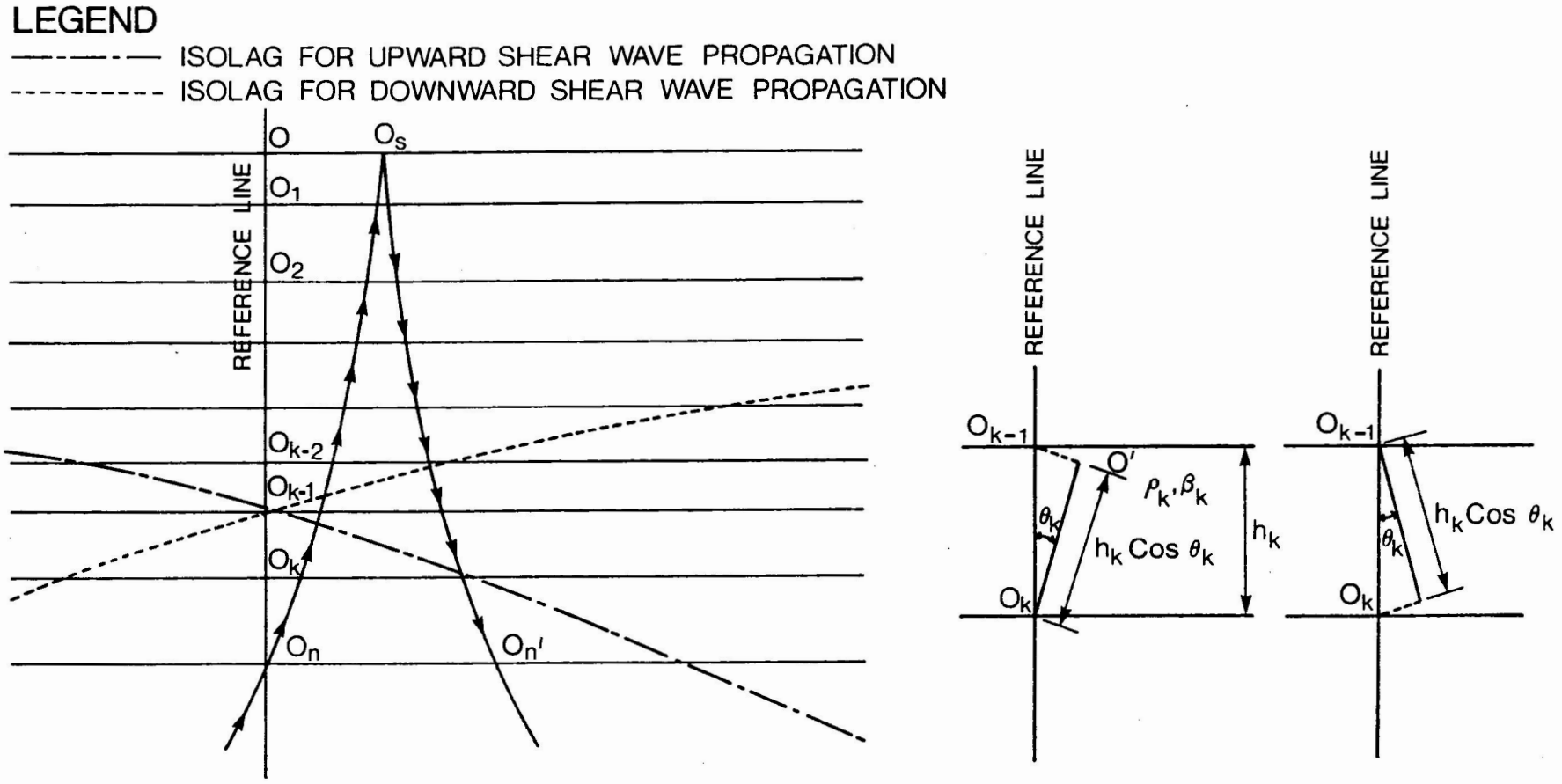

a. IDEALIZED PATH OF INCLINED SHEAR WAVE PROPAGATION IN SOIL LAYERS AND ISOLAGS

b. TIME LAG BETWEEN TOP AND BOTTOM INTERFACES OF LAYER k ALONG A VERTICAL DUE TO UPWARD AND DOWNWARD MOTIONS

FIG. 4 INCLINED SHEAR WAVE PROPAGATION THROUGH SOIL LAYERS

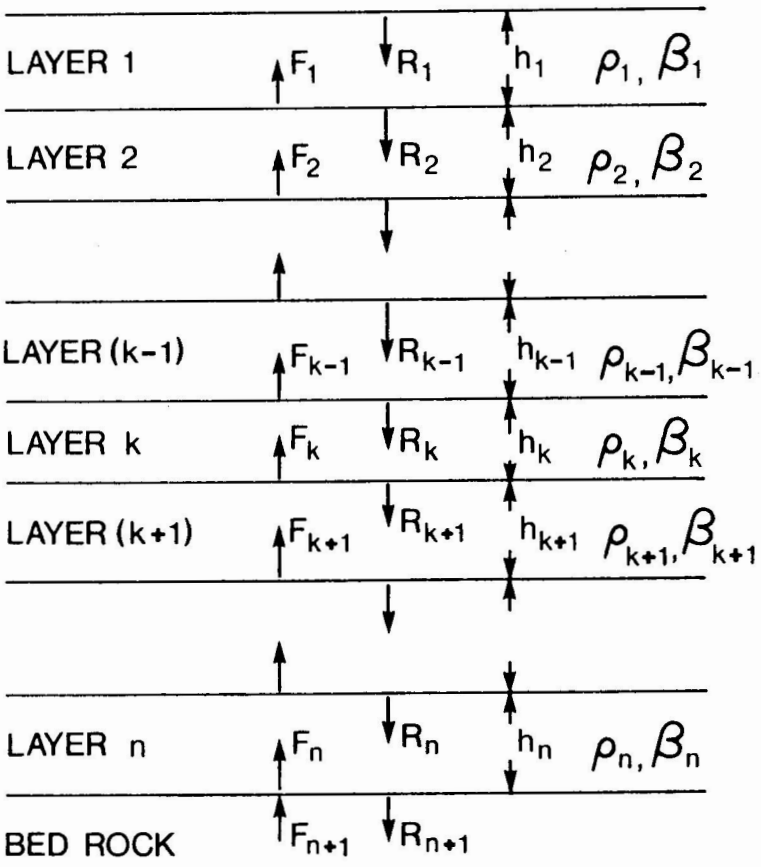

a. BED ROCK TO SURFACE RESPONSE IN LAYERED SOIL

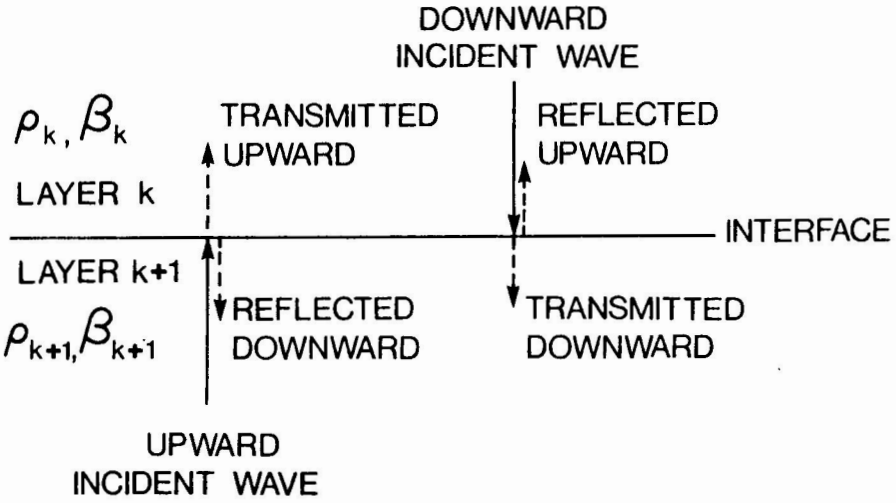

b. INCIDENT AND EMITTED SIGNALS AT A TYPICAL INTERFACE

FIG. 5 BEDROCK TO SURFACE RESPONSE IN LAYERED SOILS

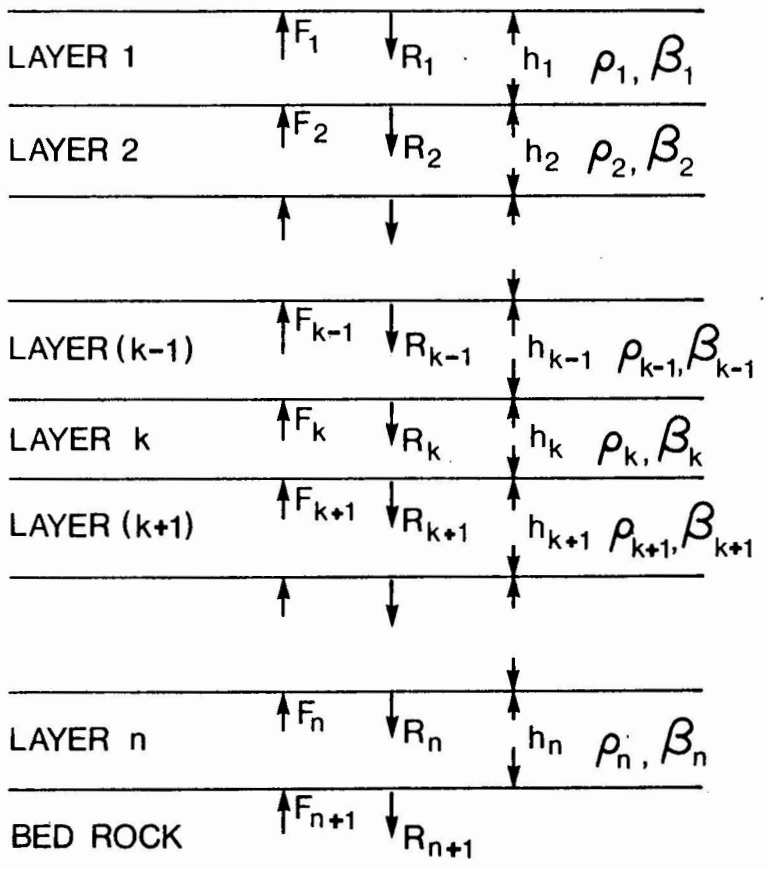

FIG. 6 SURFACE TO BEDROCK RESPONSE IN LAYERED SOILS

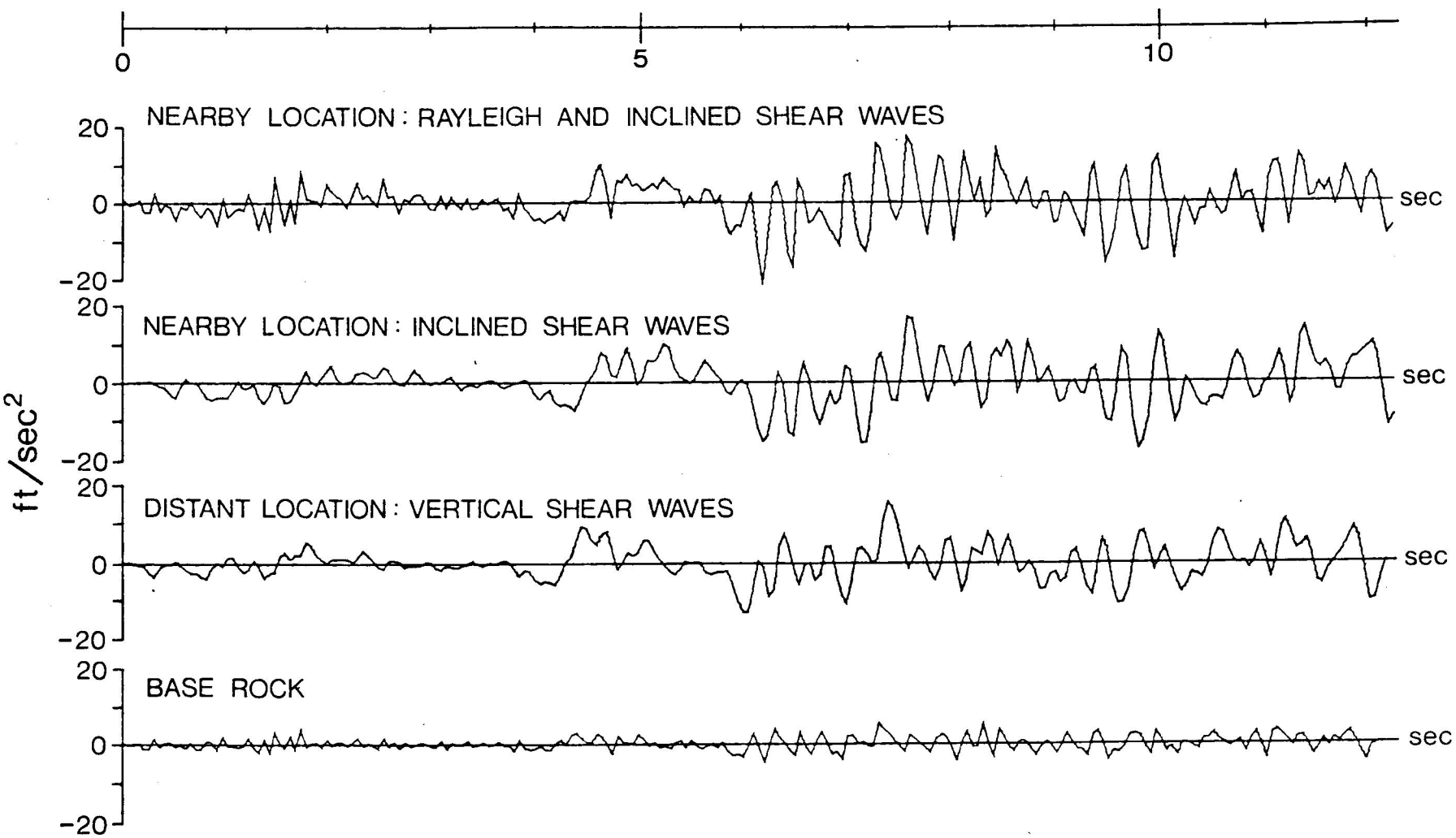

FIG. 7 SURFACE RESPONSES UNDER DIFFERENT WAVE PROPAGATION ASSUMPTIONS
(1 FT/SEC^2 = 0.3 M/SEC^2)

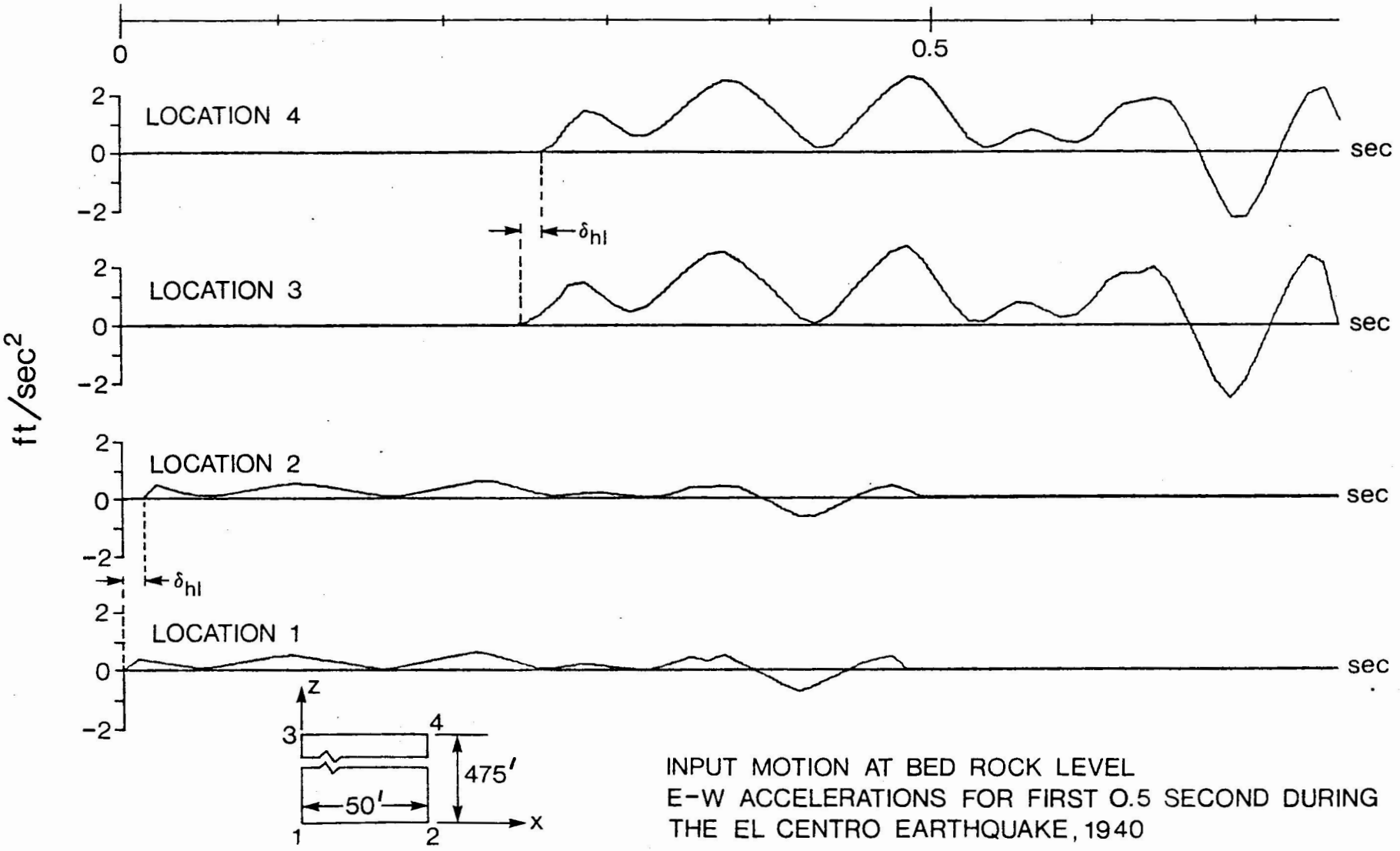

FIG. 8 SPATIAL MOTIONS FOR THREE-LAYER SYSTEM
(1 FT/SEC^2 = 0.3 M/SEC^2)

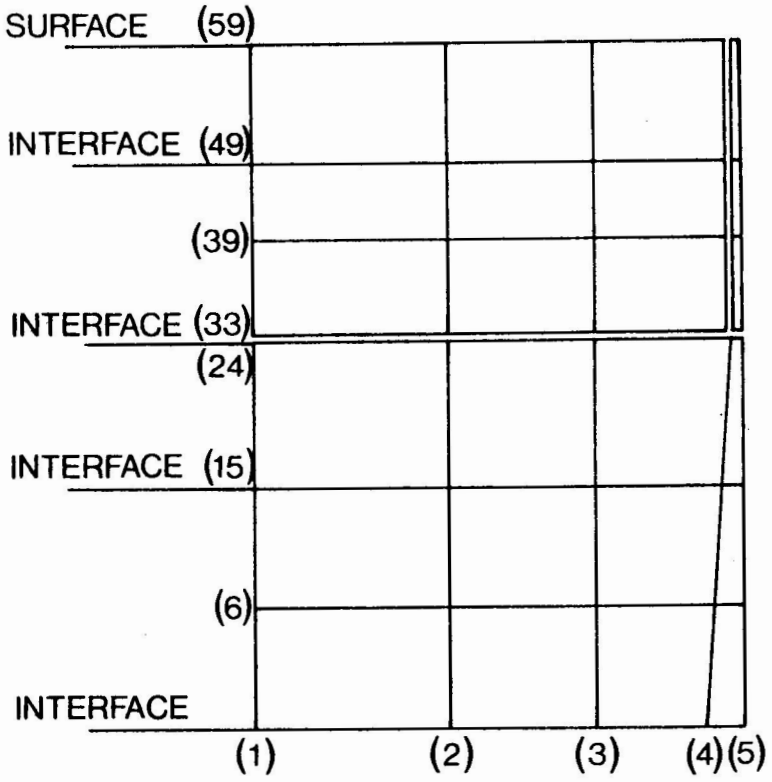

a. BOUNDARY NODES OF THE SYSTEM

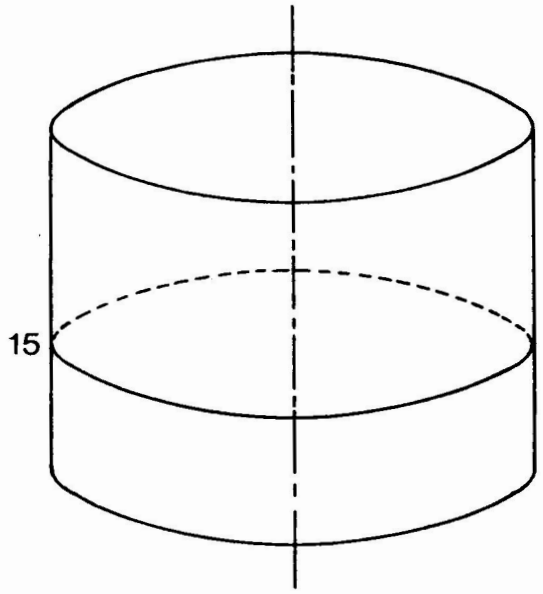

b. NODAL RING 15

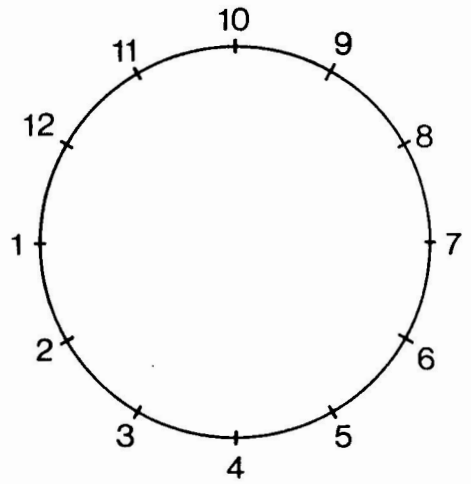

c. SELECTED POINTS ALONG NODAL RING

FIG. 9 BOUNDARY NODES OF PILE AND SELECTED POINTS ALONG NODAL RING

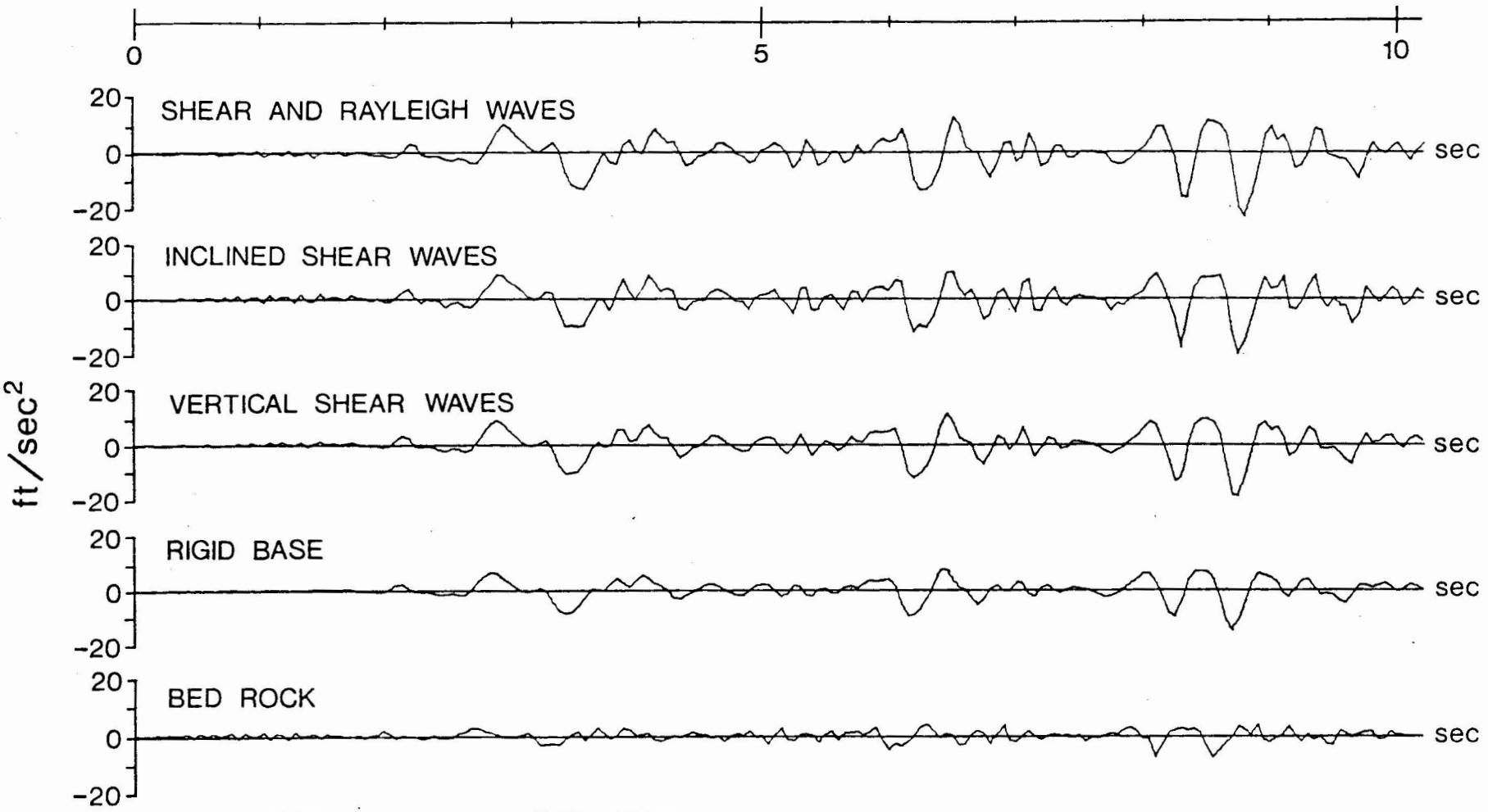

FIG. 10 PILE CAP RESPONSES UNDER DIFFERENT WAVE PROPAGATION ASSUMPTIONS
(1 FT/SEC^2 = 0.3 M/SEC^2)

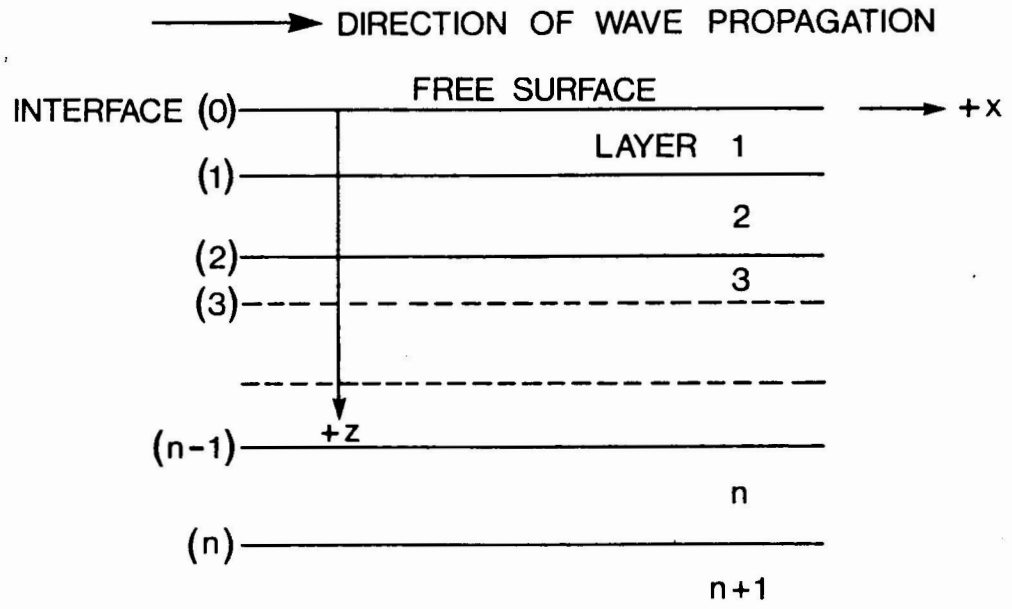

FIG. 11 LAYERS, INTERFACES AND DIRECTION OF RAYLEIGH WAVE PROPAGATION